

**SUPPLEMENTARY DATA**

for

Mode of interaction of the signal-transducing protein EIIA<sup>Glc</sup> with  
the maltose ABC transporter in the process of inducer exclusion

Steven Wuttge, Anke Licht, Mohammad Hadi Timachi, Enrica Bordignon, and

Erwin Schneider

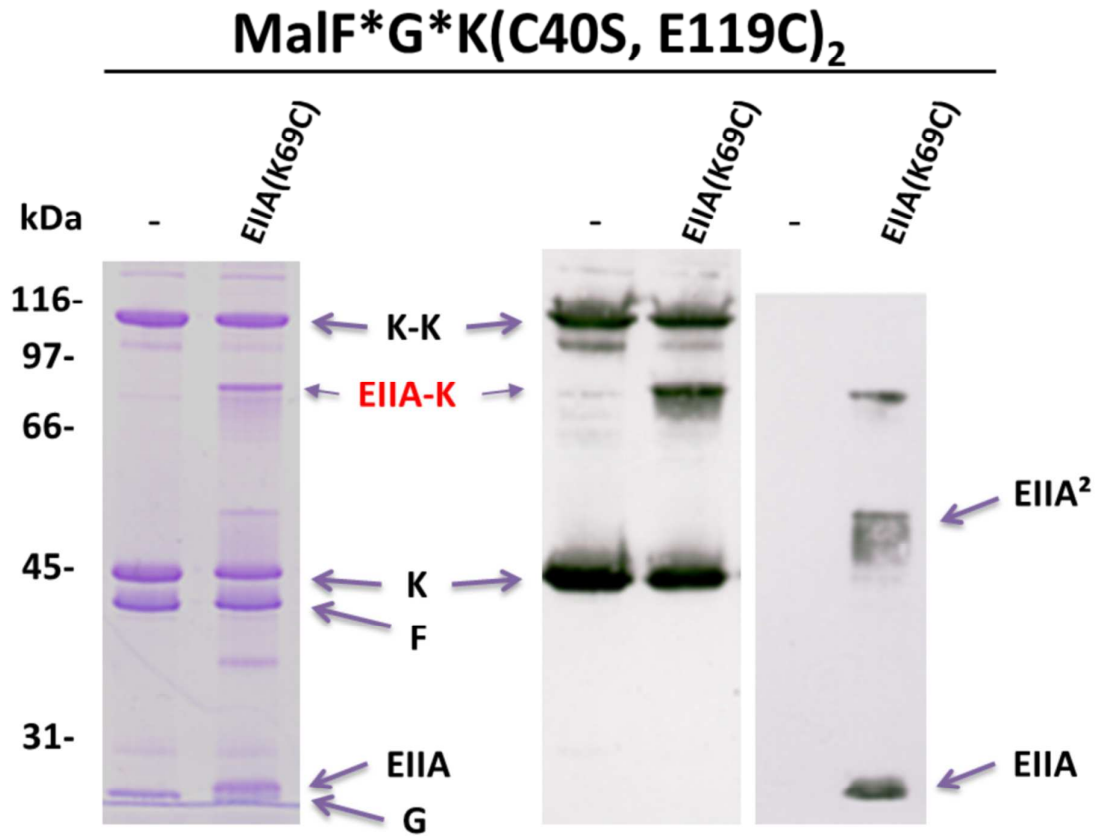


**Fig. S1. CuPhe-induced cross-linking of MalF\*G\*K(C40S, E119C)<sub>2</sub> with  $EIIA^{Glc}(K69C)$ .** Crosslinking was performed in the presence of CuPhe as described in 'Experimental procedures' and the products were analysed by SDS-PAGE (*left panel*) and immunoblots probed with anti-MalK antibodies (*center panel*) and anti- $EIIA^{Glc}$  antibodies (*right panel*).

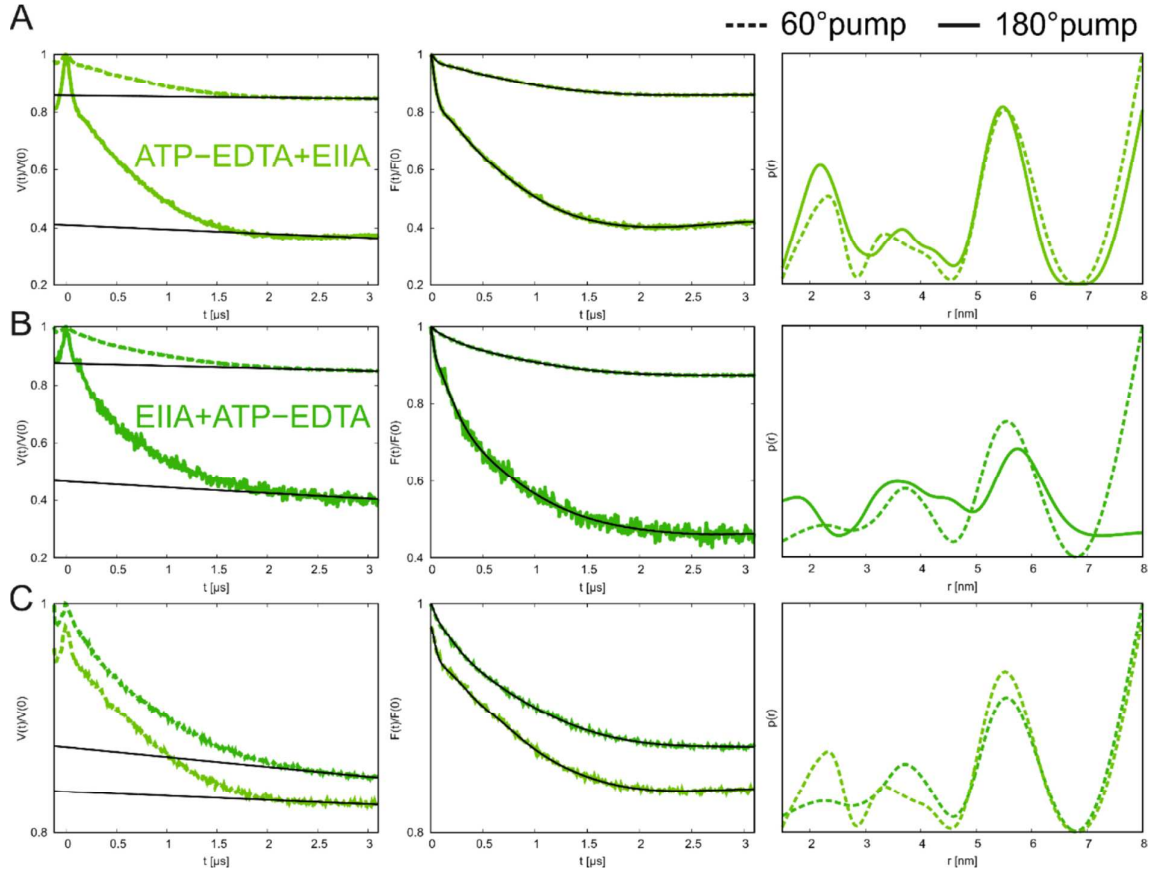


**Fig. S2. Ghost peak suppression in DEER traces.** Q-band DEER primary data  $[V(t)/V(0)]$  with fitted background (left), background-corrected DEER traces  $[F(t)/F(0)]$  with fitted distribution function (center) and corresponding distance distribution (*right*) calculated using DeerAnalysis2015 for the spin-labeled pair 17MalK/128MalK. Traces are shown for samples with EIIA<sup>Glc</sup> added before (dark green, as in Fig. 4B) or after (light green, as in Fig. 4C) ATP-EDTA. Traces were obtained using a  $\pi$  pulse in the pump frequency (panels A, B solid lines) as in Figs. 4 panels B-C or a  $\pi/3$  pulse (panels A, B dashed lines). The latter setup strongly decreases the modulation depth of the DEER traces and minimizes the artefacts exerted by the ghost peaks in a 4-spin system<sup>1,2</sup>. Negligible effects of ghost peak artefacts are present in the distance range 1.5-4 nm, which reports the opening and closing of the NBDs. (C) Comparison of the traces obtained with the  $\pi/3$  pulse for the samples pre- or post- incubated with EIIA<sup>Glc</sup>. The results are consistent with those presented in Fig. 4.

### **Supplementary References**

(1) von Hagens, T., Polyhach, Y., Sajid, M., Godt, A., and Jeschke, G. (2013) Suppression of ghost distances in multiple-spin double electron-electron resonance, *Phys Chem Chem Phys* 15,5854-5866.

(2) Valera, S., Ackermann, K., Pliotas, C., Huang, H., Naismith, J.H., and Bode, B.E. (2016) Accurate Extraction of Nanometer Distances in Multimers by Pulse EPR, *Chemistry* 22, 4700-4703.

**Table S1. Strains and plasmids used in this study**

Strain/Plasmid	Relevant genotype	Reference/Source
<i>Strain</i>		
<i>E. coli</i> JM109	e14 <sup>-</sup> ( <i>mcrA</i> ) <i>recA1</i> <i>endA1</i> <i>gyrA96</i> <i>thi-1</i> <i>hsdR17</i> ( <i>rk<sup>-</sup></i> , <i>mk<sup>+</sup></i> ) <i>supE44</i> <i>relA1</i> $\Delta$ ( <i>lac-proAB</i> ) F'[ <i>traD36</i> <i>proAB<sup>+</sup></i> <i>lacI<sup>f</sup></i> <i>lacZ</i> $\Delta$ M15]	Stratagene (La Jolla, USA)
<i>E. coli</i> BL21(DE3) $\Delta$ <i>pts</i>	<i>hsdS</i> <i>gal</i> ( $\lambda$ <i>clts857</i> <i>ind1</i> S <i>am7</i> <i>nin5</i> <i>lacUV-T7</i> <i>gene 1</i> ) $\Delta$ <i>pts43crr::kan<sup>R</sup></i>	[22]
<i>Plasmid</i>		
pAL66	<i>malK</i> (C40S, C350M, C360M, V17C, E128C), derivative of pMG39	[32]
pBB04	<i>crr</i> on pET15b, Ap <sup>R</sup>	[28]
pBB04(F88Q)	<i>crr</i> (F88Q) derivative of pBB04	[28]
pBB04(K130C)	<i>crr</i> (K130C) derivative of pBB04	Lab collection
pBK02	<i>malK</i> (C40S, Q122C), derivative of pMM37	Lab collection
pBK04	<i>malK</i> (C40S, R322C), derivative of pMM37	Lab collection
pBK05	<i>malK</i> (C40S, A320C), derivative of pMM37	Lab collection

pCB6	<i>malE</i> on pQE9, p <sub>T5</sub> , Ap <sup>R</sup>	[39]
pET15b	p <sub>T7lac</sub> ; His <sub>6</sub> -coding sequence (5'), thrombin cleavage site, Ap <sup>R</sup>	Novagen (Bad Soden, Germany)
pHL04	<i>crr</i> (P125C), derivative of pBB04	Lab collection
pHL09	<i>malK</i> (C40S, E119C), derivative of pMM37	Lab collection
pMG39	<i>malK</i> (C40S, C350M, C360M) on pSU19	Lab collection
pMM34	<i>malF</i> ( <i>cys</i> <sup>-</sup> ) <i>malG</i> ( <i>cys</i> <sup>-</sup> ) on pTZ18R	Lab collection
pMM37	<i>malK796</i> (C40S) on pSU19	[37]
pTZ18R	Phagemid, p <sub>tac</sub>	GE Healthcare
pWS02	<i>crr</i> (K69C), derivative of pBB04	This study
pWS08	<i>crr</i> (Δ1-16, P125C), derivative of pBB04	This study
pWS09	<i>Crr</i> (E97C), derivative of pBB04	This study
pWS19	<i>crr</i> (Δ1-16, K69C), derivative of pBB04	This study
pWS29	<i>crr</i> (E160C), derivative of pBB04	This study

**Table S2. C<sub>β</sub>- C<sub>β</sub> distances determined from the X-ray structure of the maltose transporter complexed with EIIA<sup>Glc</sup> (PDB code 4JBW).**

Residues		C <sub>β</sub> - C <sub>β</sub> distance (Å)
MalK	EIIA <sup>Glc</sup>	
E119	K69	10.8
E119	E160	30.5
Q122	K69	12.5
Q122	E97	14.0
A320	P125	15.4
R322	P125	14.8

**Table S3. ATPase activities of maltose transporter variants.**

Complex variant	ATPase activity <sup>a</sup> ( $\mu\text{mol P}_i \text{ mg}^{-1} \cdot \text{min}^{-1}$ )
MalF*G*K(C40S) <sub>2</sub>	1.81 $\pm$ 0.22
MalF*G*K(C40S, E119C) <sub>2</sub>	1.72 $\pm$ 0.14
MalF*G*K(C40S, Q122C) <sub>2</sub>	1.46 $\pm$ 0.12
MalF*G*K(C40S, A320C) <sub>2</sub>	1.42 $\pm$ 0.09
MalF*G*K(C40S, R322C) <sub>2</sub>	1.52 $\pm$ 0.10

<sup>a</sup> ATPase activities of transport complexes reconstituted in proteoliposomes were measured in the presence of MalE/maltose as described in 'Experimental procedures'. The values are the mean of three independent trials with SD corrected for the activity in the absence of MalE/maltose which was below 10%. \* denotes cysless subunit.



**Table S4. Inhibition (%) of ATPase activities of maltose transporter mono-cys variants by mono-cys EIIA<sup>Glc</sup> mutants**

complex variant	EIIA <sup>Glc</sup> (wt)	EIIA <sup>Glc</sup> (K69C)	EIIA <sup>Glc</sup> (E97C)	EIIA <sup>Glc</sup> (P125C)	EIIA <sup>Glc</sup> (E160C)
MalF*G*K(C40S) <sub>2</sub>	73 ± 12	64 ± 8	65 ± 7	72 ± 8	68 ± 7
MalF*G*K(C40S, E119C) <sub>2</sub>	64 ± 9	63 ± 6	52 ± 9	61 ± 8	64 ± 4
MalF*G*K(C40S, Q122C) <sub>2</sub>	59 ± 7	54 ± 5	67 ± 5	56 ± 5	55 ± 5
MalF*G*K(C40S, A320C) <sub>2</sub>	14 ± 2	12 ± 2	11 ± 2	12 ± 3	11 ± 2
MalF*G*K(C40S, R322C) <sub>2</sub>	0	0	0	0	0

ATPase activities of the transporter variants in the absence of EIIA<sup>Glc</sup> (see Table S3) were set 100 %. Values are the mean of three independent trials with SD. nd, not determined. \*denotes cysless subunit.

**Table S5. ATPase activities of MalF\*G\*K(V17C, E128C) embedded in nanodiscs in the absence and presence of EIIA<sup>Glc</sup>**

<b>Transporter complex</b>	<b>No addition</b>	<b>+ MalE/maltose</b>	<b>+ MalE/maltose/ EIIA<sup>Glc</sup></b>	<b>+ MalE/maltose/ EIIA<sup>Glc</sup>(F88Q)</b>
MalF*G*K* <sub>2</sub>	0.04 ± 0.02	3.31 ± 0.18	0.54 ± 0.02	3.44 ± 0.27
MalF*G*K(V17C/E128C) <sub>2</sub> + DTT	0.04 ± 0.01	3.53 ± 0.19	0.59 ± 0.14	3.88 ± 0.14
MalF*G*K(V17R1/E128R1) <sub>2</sub>	0.03 ± 0.01	3.18 ± 0.15	0.72 ± 0.09	3.37 ± 0.18

ATPase activities of purified complex variants in nanodiscs (0.5 μM) were measured in the absence or presence of MalE (5 μM) and maltose (10 μM). Nanodiscs were prepared as described in ‘Experimental procedures’. Data represent means of at least three independent experiments. \*denotes cys-less subunit, R1 denotes the spin-labeled side chain. Due to an internal cross-link the MalF\*G\*K(V17C/E128C)<sub>2</sub> complex was assayed in the presence of 1 mM DTT.